Magnetoelectric effects due to elastic coupling in ferroelectric/ferromagnetic multilayers

Biao Wang[1,a] and C. H. Woo[2]
[1]*State Key Laboratory of Optoelectronic Materials and Technologies, Institute of Optoelectronic and Functional Composite Materials, and School of Physics and Engineering, Sun Yat-sen University, Guangzhou 510275, People's Republic of China*
[2]*Department of Electronic and Information Engineering, The Hong Kong Polytechnic University, Hong Kong, Hong Kong SAR, People's Republic of China*

(Received 3 November 2007; accepted 13 April 2008; published online 18 June 2008)

The critical behavior of a multilayered system of alternating ferroelectric and ferromagnetic thin films on a substrate of finite thickness is studied. A thermodynamic approach via the Ginzburg–Landau formulation is followed. Our interest is in the magnetoelectric effects exhibited in the critical behavior of the multilayer system, caused by the interlayer elastic interaction. The system is characterized by two bifurcation points. The system exhibits the strongest magnetoelectric effect near the second bifurcation. © *2008 American Institute of Physics*. [DOI: 10.1063/1.2939580]

I. INTRODUCTION

Multiferroic material or material systems are characterized by their interacting ferroelectric, ferromagnetic, and ferroelastic properties derived from the coupling of two or more of the electric, magnetic, and structural order parameters. These systems are of interest to both the academic and engineering communities due to their attractive and unique properties, which make them useful in information storage, multifunctional electronic devices, etc.

The magnetoelectric effect was predicted by Curie in 1894, and subsequently observed by Astrov[1] in Cr_2O_3 in 1960. Recent progress in thin-film growth and other sample preparation techniques made the fabrication of the next-generation multifunctional devices possible and contributed considerably to their renaissance. Despite active research, there is only a limited choice of single-phase materials exhibiting coexistence of strong ferro-/ferrimagnetism and ferroelectricity.[2,3] van Suchtelen[4] proposed that composites of piezoelectric and magnetostrictive phases can be magnetoelectrically coupled. Recent development focuses on various multiferroic composites with large ferroelectromagnetic material constants.[5,6] Wang *et al.*[7] investigated heteroepitaxially constrained thin films of the ferroelectromagnet, $BiFeO_3$, and they found a significant enhancement of magnetization and polarization in the thin film. Zheng *et al.*[8] investigated the coupling between ferroelectric and ferromagnetic order parameters in a nanostructured $BaTiO_3$–$CoFe_2O$ ferroelectromagnetic composite. They found that the magnetoelectric coupling in such nanostructure can be understood on the basis of the strong elastic interactions between the two phases. Efremov *et al.*[9] proposed a new route to utilize the coupling between magnetic and charge ordering to obtain ferroelectric magnets. Fiebig *et al.*[10] reported spatial maps of coupled antiferromagnetic and ferroelectric domains in $YMnO_3$, obtained by imaging with optical second harmonic generations. Recently, the first-principles simulation was used to predict ferroelectric and ferromagnetic couplings in multiferroic materials.[11–13] Murugavel *et al.*[14,15] used the pulse-laser deposition technique to fabricate a series of superlattices and trilayers composed of ferromagnetic and ferroelectric layers and investigated their properties. Nan and co-workers[16,17] found giant megneto-electric responses in multiferroic polymer-based composites.

The foregoing suggests that electric and magnetic effects can be strongly coupled via the interacting elastic stresses introduced through piezoelectric and piezomagnetic properties in multiferroic material systems. The resulting magneto-electric coupling will most likely manifest itself through the highly sensitive critical phenomena. The purpose of the present paper is to investigate the critical behavior of a multilayered system of alternating ferroelectric and ferromagnetic thin films on a finite substrate along this line of thought. The dynamics of the system is formulated and analyzed via a thermodynamic approach using the Ginzburg–Landau free energies of the bulk ferroelectric and ferromagnetic materials.

II. THERMODYNAMIC MODEL OF A MULTIFERROIC-LAYERED THIN-FILM SYSTEM

We consider a multilayer thin-film system with alternating ferroelectric and ferromagnetic components of thicknesses h_e and h_m, respectively, on substrates of finite thickness H on both sides of the system, half of which is shown in Fig. 1. We use self-polarization[18,19] (i.e., the spontaneous polarization of a sample in the absence of any applied field—electric, magnetic, and mechanical) in the ferroelectric layers as an order parameter of the system to describe the dynamic behavior of the para-/ferroelectric phases. Specifically, the depolarization field is considered to be an applied field. The rigorous thermodynamic origin of this formulation has been the subject of Ref. 19, according to which the dynamics of the total polarization (self + induced) in the presence of the applied fields can be retrieved from that of the self-polarization. Without loss of generality, we only consider the

[a]Electronic mail: wangbiao@mail.sysu.edu.cn.

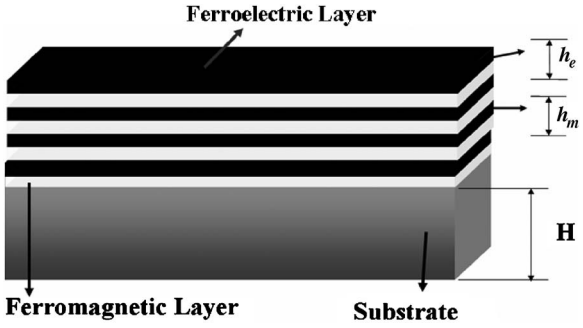

FIG. 1. Schematic of a symmetric half of the multiferroic superlattice composed of alternating ferroelectric and ferromagnetic layers.

component of P of the self-polarization perpendicular to the film surface, as in our previous work.[18] The total free energy f of the ferroelectric layers can be expressed in terms of a sum of contributions f_P, f_e^{el}, and f_e^{Σ},

$$f_e = f_P + f_e^{\mathrm{el}} + f_e^{\Sigma},$$

where f_e^{el} and f_e^{Σ} are the elastic and surface contributions, respectively. In terms of the Ginzburg–Landau model, the contribution due to the self-polarization f_p can be written as

$$f_P = n_e \int \int_{V_e} \int \left[\frac{A_e}{2}(T - T_{c0}^e)P^2 - \frac{1}{2}E_d P + \frac{B_e}{4}P^4 + \frac{C_e}{6}P^6 + \frac{D_e}{2}\left(\frac{\partial P}{\partial z}\right)^2 \right] dv = n_e \int_{-h_e/2}^{h_e/2} \left[\frac{A_e}{2}(T - T_{c0}^e)P^2 - \frac{1}{2}E_d P + \frac{B_e}{4}P^4 + \frac{C_e}{6}P^6 + \frac{D_e}{2}\left(\frac{\partial P}{\partial z}\right)^2 \right] dz, \quad (1)$$

where T_{c0}^e is the critical temperature for the corresponding bulk material, and A_e, B_e, C_e, and D_e are the Ginsberg–Landau expansion coefficients for the bulk material. n_e is the total number of ferroelectric layers, each of which has a unit surface area and a volume V_e. E_d is the depolarization field. Since the layer is assumed to be infinite along the x- and y-directions, the polarization is only a function of z along the thickness direction. In terms of the self-polarization, it can be shown[18,19] that $E_d = -P/\varepsilon$, where ε is the dielectric constant of the ferroelectric layers. We note that E_d can also be expressed in terms of the total polarization by replacing ε with the vacuum dielectric constant (see Ref. 18). To cover ferroelectric materials that undergo first-order transitions, we have added the term $C_e/6P^6$ in the expansion.

Similarly, the dynamics of the ferromagnetic layers is described using the self-magnetization M as an order parameter. Considering that the transformation strain is mainly along the magnetization direction, we only consider the component M along the x-direction in the film plane. This is in contrast to the ferroelectric layers where materials such as perovskites have their transformation strains mainly in the transverse directions. With the spontaneous polarization along the z-direction and the spontaneous magnetization along the x- or y-direction, the most significant magnetoelectric interactions can be produced through the elastic strains. The assumption is also consistent with experimental observations. The total free energy f_m of the ferromagnetic layers can be expressed similarly to the ferroelectric layers,

$$f_m = f_M + f_m^{\mathrm{el}} + f_m^{\Sigma},$$

where f_m^{el} and f_m^{Σ} are the elastic and the surface or interface contributions. Our interest in this work concentrates on the coupling of the ferromagnetic and the ferroelectric transitions through their sizable transformation strains. We therefore neglect effects such as those due to the change in the electronic structure near the interface, etc. Similar to the ferroelectric layers, the contribution due to the self-magnetization f_M is also written in terms of the Ginzburg–Landau functional as

$$f_M = n_m \int \int_{V_m} \int \left[\frac{A_m}{2}(T - T_{c0}^M)M^2 + \frac{B_m}{4}M^4 + \frac{D_m}{2}\left(\frac{\partial M}{\partial z}\right)^2 \right] dv = n_m \int_{-h_m/2}^{h_m/2} \left[\frac{A_m}{2}(T - T_{c0}^M)M^2 + \frac{B_m}{4}M^4 + \frac{D_m}{2}\left(\frac{\partial M}{\partial z}\right)^2 \right] dz, \quad (2)$$

where the parameters can be defined similarly as in Eq. (1). We only expand to $B_m/4M^4$ in this case since most ferromagnetic transitions are second order.

The multilayer system we are considering is elastically inhomogeneous. The elastic energy of the system must be calculated, taking into account the mechanical equilibrium of the system under the action of electrostrictive and magnetostrictive forces and obeying the condition of total system integrity, i.e., mechanical compatibility of the ferroelectric, ferromagnetic, and substrate layers. The elastic contribution f_{el} to the total free energy is thus given by a sum of three contributions from the ferroelectric and ferromagnetic thin films and the substrate, respectively,

$$f_{\mathrm{el}} = \frac{1}{2}n_e \mathbf{C}^E \int_{-h_e/2}^{h_e/2} (\boldsymbol{\varepsilon}^{0E} - \boldsymbol{\varepsilon}^{Et} + \boldsymbol{\varepsilon}^{S})^2 dz + \frac{1}{2}n_m \mathbf{C}^M \int_{-h_m/2}^{h_m/2} (\boldsymbol{\varepsilon}^{0M} - \boldsymbol{\varepsilon}^{Mt} + \boldsymbol{\varepsilon}^{S})^2 dz + \frac{1}{2}H\mathbf{C}^0(\boldsymbol{\varepsilon}^{S})^2, \quad (3)$$

where $\boldsymbol{\varepsilon}^{0E}$ and $\boldsymbol{\varepsilon}^{0M}$ are the misfit strains relative to the substrate in the ferroelectric and ferromagnetic layers, respectively. $\boldsymbol{\varepsilon}^{S}$ is the induced elastic strain in the substrate layer. $\mathbf{C}^E$, $\mathbf{C}^M$, and $\mathbf{C}^0$ are the corresponding elastic moduli. $\boldsymbol{\varepsilon}^{Et}$ and $\boldsymbol{\varepsilon}^{Mt}$ are the eigenstrains of ferroelectric and ferromagnetic transformations, respectively, from which the electrostrictive and magnetostrictive forces originate.

Denoting the nonzero components of the misfit strains along the x- and y-directions by $\boldsymbol{\varepsilon}_{11}^{0E}$, $\boldsymbol{\varepsilon}_{22}^{0E}$ and $\boldsymbol{\varepsilon}_{11}^{0M}$, $\boldsymbol{\varepsilon}_{22}^{0M}$, respectively, and assuming that the multilayer system is grown heteroepitaxially from a substrate, $\boldsymbol{\varepsilon}_{\alpha\alpha}^{0E}$ and $\boldsymbol{\varepsilon}_{\alpha\alpha}^{0M}$ can be expressed as usual in terms of the lattice constants of the films a_α^{Ef} and a_α^{Mf} and substrate a_α^{s},

$$\boldsymbol{\varepsilon}_{\alpha\alpha}^{0E}=\frac{a_\alpha^s-a_\alpha^{Ef}}{a_\alpha^{Ef}},\boldsymbol{\varepsilon}_{\alpha\alpha}^{0M}=\frac{a_\alpha^s-a_\alpha^{Mf}}{a_\alpha^{Mf}}. \tag{4}$$

In deriving Eq. (4), we assume that the misfit strains are uniform within each layer and the strains are equal in all layers.

The transformation eigenstrains in Eq. (3) can be written in terms of the order parameters P and M via the electrostrictive and magnetostrictive (volumetric plus anisotropic) coefficients $\mathbf{Q}$ and $\mathbf{Q}_m$, using the relations $\boldsymbol{\varepsilon}^{Et}(z)=\mathbf{Q}P^2(z)$ and $\boldsymbol{\varepsilon}^{Mt}(z)=\mathbf{Q}_mM^2(z)$, respectively.

We note that it is only when the substrate is infinitely thick or rigid that the misfit and transformation strains within each layer are exactly balanced by the elastic strains across neighboring layers. Transformation strains cannot be transmitted via misfit strains across neighboring layers in such cases. In our case of a compliant substrate, however, the constraint is much weakened, allowing transformations to interact across neighboring layers. If the substrate disappears, one should observe the strongest magnetoelectric coupling.

A. Elastic coupling

The elastic strains of the substrate in Eq. (3) can be calculated by adopting the Timoshenko and Gooier[20] method for thermal stresses. We recall that the configuration being considered is symmetrical, with no bending. In the present approach, the ferroelectric, ferromagnetic, and substrate layers interact via the conditions of mechanical equilibrium and compatibility (sample integrity). The assumption of uniform strain is adopted, although in reality, the strain in each layer of the inhomogeneous sample must be graded along the thickness. Nevertheless, what is neglected is a higher order contribution. The present treatment should suffice for our purpose.

Thus, the compatibility condition of the multilayer system requires stresses $\sigma_{ij}^E=C_{ijkl}^E(\varepsilon_{kl}^{0E}-\varepsilon_{kl}^{Et})$ and $\sigma_{ij}^M=C_{ijkl}^M(\varepsilon_{kl}^{0M}-\varepsilon_{kl}^{Mt})$ on the ferroelectric and ferromagnetic layers, respectively. These stresses create a resultant force at the ends of the plates, given by

$$F_\alpha=n_e\int_{-h_e/2}^{h_e/2}\sigma_{\alpha\alpha}^E dz+n_m\int_{-h_m/2}^{h_m/2}\sigma_{\alpha\alpha}^M dz,\quad \alpha=1,2. \tag{5}$$

That is,

$$\mathbf{F}=n_e\int_{-h_e/2}^{h_e/2}\boldsymbol{\sigma}^E dz+n_m\int_{-h_m/2}^{h_m/2}\boldsymbol{\sigma}^M dz. \tag{6}$$

For the entire substrate and film system to remain in equilibrium a force equal and opposite to $\mathbf{F}$ must be applied. If the system is not symmetrical, the balancing force will introduce a bending moment. To simplify our analysis, the system is assumed to be symmetrical and the bending moment can be neglected. $\boldsymbol{\varepsilon}^S$ is then the uniform strain produced in the substrate by the balancing force. At final equilibrium the strain $\boldsymbol{\varepsilon}^S$ will be applied to the entire system (i.e., including the substrate). Then, the corresponding balancing equation can be written as

$$n_eh_e\boldsymbol{\sigma}^{Eb}+n_mh_m\boldsymbol{\sigma}^{Mb}+H\boldsymbol{\sigma}^{Sb}=-\mathbf{F}, \tag{7}$$

with

$$\boldsymbol{\sigma}^{Eb}=\mathbf{C}^E\boldsymbol{\varepsilon}^S,\boldsymbol{\sigma}^{Mb}=\mathbf{C}^M\boldsymbol{\varepsilon}^S,\boldsymbol{\sigma}^{Sb}=\mathbf{C}^0\boldsymbol{\varepsilon}^S. \tag{8}$$

In terms of $\boldsymbol{\varepsilon}^S$, Eqs. (7) and (8) can be written as

$$(n_eh_e\mathbf{C}^E+n_mh_m\mathbf{C}^M+H\mathbf{C}^0)\boldsymbol{\varepsilon}^S=-\mathbf{F} \tag{9}$$

from which $\boldsymbol{\varepsilon}^S$ is linearly related to $\mathbf{F}$ via a constant system compliance $\boldsymbol{\Xi}$,

$$\boldsymbol{\varepsilon}^S=-\boldsymbol{\Xi}\mathbf{F}\ \text{ with }\ \boldsymbol{\Xi}\equiv[n_eh_e\mathbf{C}^E+n_mh_m\mathbf{C}^M+H\mathbf{C}^0]^{-1}. \tag{10}$$

If we define a force-constant matrix $\mathbf{K}$ by $K_{\alpha\beta}=n_eh_eC_{\alpha\beta}^E+n_mh_mC_{\alpha\beta}^M+HC_{\alpha\beta}^0$, both $\mathbf{K}$ and $\boldsymbol{\Xi}$ are real and symmetric. As an example, in the particular case of isotropic elasticity,

$$\begin{Bmatrix}\varepsilon_1^S\\ \varepsilon_2^S\end{Bmatrix}=\frac{-1}{\|\mathbf{K}\|}\begin{Bmatrix}K_{11} & -K_{12}\\ -K_{12} & K_{11}\end{Bmatrix}\begin{Bmatrix}F_1\\ F_2\end{Bmatrix}. \tag{11}$$

Thus, from Eqs. (6) and (10), we can write

$$\begin{aligned}\boldsymbol{\varepsilon}^S&=-n_e\boldsymbol{\Xi}\int_{-h_e/2}^{h_e/2}\boldsymbol{\sigma}^E dz-n_m\boldsymbol{\Xi}\int_{-h_m/2}^{h_m/2}\boldsymbol{\sigma}^M dz\\&=-n_e\boldsymbol{\Xi}\mathbf{C}^E\\&\quad\times\int_{-h_e/2}^{h_e/2}(\boldsymbol{\varepsilon}^{0E}-\boldsymbol{\varepsilon}^{Et})dz-n_m\boldsymbol{\Xi}\mathbf{C}^M\int_{-h_m/2}^{h_m/2}(\boldsymbol{\varepsilon}^{0M}\\&\quad-\boldsymbol{\varepsilon}^{Mt})dz.\end{aligned} \tag{12}$$

The substitution of Eq. (12) into Eq. (3) yields an interaction term between the ferroelectric and ferromagnetic layers through the elastic strain induced in the substrate, which produces a magnetoelectric coupling. To derive the dynamic equation of the system, we need to calculate the functional variation of the elastic energy with respect to the polarization and magnetization. Thus,

$$\delta_Pf_{\text{el}}=\int_{-h_e/2}^{h_e/2}[n_e\alpha^E(\langle P^2\rangle,\langle M^2\rangle)P(z)+n_e\beta^EP^3(z)]\delta Pdz, \tag{13}$$

where $\langle P^2\rangle=\int_{-h_e/2}^{h_e/2}P^2dz$ and $\langle M^2\rangle=\int_{-h_m/2}^{h_m/2}M^2dz$.

In Eq. (13), α^E and β^E can be written in the form

$$\alpha^E(\langle P^2\rangle,\langle M^2\rangle)\equiv\alpha_0^E+\alpha_p^E\langle P^2\rangle+\alpha_m^E\langle M^2\rangle\quad\text{and}\quad\beta^E\equiv 2C_{ij}^EQ_iQ_j, \tag{14a}$$

with

$$\alpha_0^E=-2Q\mathbf{C}^E\boldsymbol{\varepsilon}^{0E}+2Q\mathbf{C}^E(h_e\boldsymbol{\Xi}\mathbf{C}^E\boldsymbol{\varepsilon}^{0E}+h_m\boldsymbol{\Xi}\mathbf{C}^M\boldsymbol{\varepsilon}^{0M}), \tag{14b}$$

and α_p^E and α_m^E are defined in the same way according to Eq. (13). Similarly, we can also obtain

$$\delta_Mf_{\text{el}}=\int_{-h_m/2}^{h_m/2}[n_m\alpha^M(\langle P^2\rangle,\langle M^2\rangle)M(z)+n_m\beta^MM^3(z)]\delta Mdz, \tag{15}$$

where α^M and β^M for the magnetic layer are defined simi-

larly to α^E and β^E in Eqs. (14a) and (14b) in terms of corresponding constants α_0^M, α_p^M, and α_m^M.

It is reasonable to assume that the different electronic environment near the interfaces between the ferroelectric and ferromagnetic layers may also induce an extra contribution to the free energy. We assume that it can be expressed in terms of material constants δ_e and δ_m as

$$f_\Sigma = \int \int_S \left(\frac{P^2}{2\delta_e} + \frac{M^2}{2\delta_m} \right) ds, \tag{16}$$

where S denotes the total area of the interfaces. We note that in Eq. (16), interactions of electronic nature between films are not considered as we have mentioned earlier.

The first term in Eq. (16) has been used in the ferroelectric phase transition theory. Such a formulism has been introduced by de Gennes to empirically consider surface problems in superconductivity.[21] Generally speaking, the change in the density of states at the Fermi level on surfaces and interfaces in ferromagnetic thin films[22–24] also suggests that there should also be a change in the magnetization on the surfaces of the ferromagnetic thin films. It may therefore be proper to introduce a similar parameter δ_m to account for the interface effect on ferromagnetic phase transition.

Combining Eqs. (1)–(3) and (16), the total free energy Φ of the system can be written as

$$\Phi = f_P + f_M + f_{\text{el}} + f_\Sigma. \tag{17}$$

It is easy to see that as a result of the necessary conditions of mechanical equilibrium and compatibility on the multilayer system, an interaction of elastic origin must arise between the ferroelectric and ferromagnetic layers due to f_{el} from Eqs. (13) and (15) via the coupling constants α^E and α^M.

B. System dynamic equations

The dynamic equation of P can be derived from Eq. (17) using Eqs. (1) and (13). Thus,

$$\frac{\partial P}{\partial t} = -\mu_e \frac{\delta \Phi}{\delta P} = -\mu_e \left[A^E P + \frac{n_e}{\varepsilon} P + B^E P^3 + n_e C_e P^5 - n_e D_e \frac{\partial^2 P}{\partial z^2} \right]. \tag{18}$$

where μ_e is the kinetic coefficient related to the ferroelectric domain wall mobility and

$$A^E = n_e[A_e(T - T_{c0}^e) + \alpha_0^E + \alpha_p^E \langle P^2 \rangle + \alpha_m^E \langle M^2 \rangle] B^E = n_e(B_e + \beta^E). \tag{19}$$

Performing functional variation on the surface term in Eq. (17) yields the boundary conditions

$$\frac{\partial P}{\partial z} = \mp \frac{P}{\delta_e} \quad \text{for} \quad z = \pm \frac{h_e}{2}. \tag{20}$$

Similarly, the dynamic equation of the magnetization M in the system as derived from Eq. (17) using Eqs. (2) and (15) is

$$\frac{\partial M}{\partial t} = -\mu_m \frac{\delta \Phi}{\delta M} = -\mu_m \left[A^M M + B^M M^3 - n_m D_m \frac{\partial^2 M}{\partial z^2} \right], \tag{21}$$

where μ_m is the kinetic coefficient related to the magnetic domain wall mobility and

$$\frac{\partial M}{\partial t} = -\mu_m \frac{\delta \Phi}{\delta M} = -\mu_m \left[A^M M + B^M M^3 - n_m D_m \frac{\partial^2 M}{\partial z^2} \right], \tag{22}$$

Similarly, performing variation on the surface term in Eq. (17) yields the boundary conditions

$$\frac{\partial M}{\partial z} = \mp \frac{M}{\delta_m} \quad \text{for} \quad z = \pm \frac{h_m}{2}. \tag{23}$$

Here we assume that the phase transition process is a slow relaxation process, and we do not focus on the dynamic magnetic domain switching process.

It is clear that the polarization P and magnetization M in Eqs. (19) and (22) are coupled through α^E, α^M, β^E, and β^M, which represent the elastic interaction between the electrostrictive and magnetostrictive effects from different layers. This coupling is where the magnetoelectric effect in the present system comes from. Equations (18) and (21) have stationary solutions corresponding to stationary states P_0 and M_0. For example, the trivial solutions $P_0=0=M_0$ correspond to the stationary paraelectric and paramagnetic states. Following Wang and Woo,[18] we determine the critical conditions of the stability of the stationary states by performing a linear stability analysis on the system of Eqs. (18) and (21), and we discuss the effects of the magnetoelectric coupling strength, film thickness, etc.

We note that a local coordinate system has been used to simplify the formulation, in which the midpoint of each layer is chosen as the zero points of the z-axis.

III. PHASE STABILITY AND CRITICAL CHARACTERISTICS

The stability of a stationary state (P_0, M_0) is probed by the application of a small perturbation (Δ_e, Δ_m). Retaining only terms linear in Δ_e, Δ_m, we obtain from Eqs. (18) and (21) the evolution equations of the perturbations given by

$$\frac{\partial \Delta_e}{\partial t} = -\mu_e \left[\left(\left. \frac{\delta A^E}{\delta P} \right|_{\substack{P=P_0 \\ M=M_0}} P_0 + A^E + \frac{n_e}{\varepsilon} + 3B^E P_0^2 + \left. \frac{\delta B^E}{\delta P} \right|_{\substack{P=P_0 \\ M=M_0}} P_0^3 + 6C^E P_0^5 \right) \Delta_e + \left. \frac{\delta A^E}{\delta M} \right|_{\substack{P=P_0 \\ M=M_0}} P_0 \Delta_m + \left. \frac{\delta B^E}{\delta M} \right|_{\substack{P=P_0 \\ M=M_0}} P_0^3 \Delta_m - n_e D_e \frac{\partial^2 \Delta_e}{\partial z^2} \right], \tag{24}$$

$$\frac{\partial \Delta_m}{\partial t} = -\mu_m \Bigg[\Bigg(\left.\frac{\delta A^M}{\delta M}\right|_{\substack{P=P_0 \\ M=M_0}} M_0 + A^M + 3B^M M_0^2 + \left.\frac{\delta B^M}{\delta M}\right|_{\substack{P=P_0 \\ M=M_0}} M_0^3 \Bigg) \Delta_m + \left.\frac{\delta A^M}{\delta P}\right|_{\substack{P=P_0 \\ M=M_0}} M_0 \Delta_e + \left.\frac{\delta B^M}{\delta P}\right|_{\substack{P=P_0 \\ M=M_0}} M_0^3 \Delta_e - n_m D_m \frac{\partial^2 \Delta_m}{\partial z^2} \Bigg]. \tag{25}$$

Evaluating the variation derivatives from Eqs. (19) and (22), and taking into account that M_0 and P_0 are spatially segregated so that $M_0 P_0 \equiv 0$, the evolution equation of (Δ_e, Δ_m) can be written as

$$\frac{\partial}{\partial t}\begin{pmatrix} \Delta_e \\ \Delta_m \end{pmatrix} = -\begin{pmatrix} U_e - \mu_e n_e D_e \frac{\partial^2}{\partial z^2} & 0 \\ 0 & U_m - \mu_m n_m D_m \frac{\partial^2}{\partial z^2} \end{pmatrix} \times \begin{pmatrix} \Delta_e \\ \Delta_m \end{pmatrix}, \tag{26}$$

where

$$U_e = \mu_e \left[A^E + \frac{n_e}{\varepsilon} + (3B^E + 2n_e \alpha_p^E) P_0^2 + 6C^E P_0^5 \right],$$

$$U_m = \mu_m [A^M + (3B^M + 2n_m \alpha_m^M) M_0^2]. \tag{27}$$

Equation (26) is subject to the boundary conditions on the ferroelectric and ferromagnetic film surfaces $\pm h_e$ and $\pm h_m$, that is,

$$\frac{\partial}{\partial z}\begin{pmatrix} \Delta_e \\ \Delta_m \end{pmatrix} = -\begin{pmatrix} \mp \delta_e^{-1} & 0 \\ 0 & \mp \delta_m^{-1} \end{pmatrix}\begin{pmatrix} \Delta_e \\ \Delta_m \end{pmatrix}. \tag{28}$$

To solve for the temporal and spatial dependence of (Δ_e, Δ_m), we separate the space and time coordinates by writing

$$\begin{pmatrix} \Delta_e \\ \Delta_m \end{pmatrix} = \exp(\omega t)\begin{pmatrix} \varphi_e(z) \\ \varphi_m(z) \end{pmatrix}. \tag{29}$$

For a symmetric configuration, the condition $d\Delta_e/dz = 0, d\Delta_m/dz = 0$ at $z=0$ must also hold. Writing $\varphi_e = \cos(k_e z)$ and $\varphi_m = \cos(k_m z)$, and substituting Eq. (29) into Eq. (26), we obtain the following determinantal equation for ω:

$$\begin{Vmatrix} U_e + \mu_e n_e D_e k_e^2 + \omega & 0 \\ 0 & U_m + \mu_m n_m D_m k_m^2 + \omega \end{Vmatrix} = 0, \tag{30a}$$

which has the form

$$(\omega - \omega_>)(\omega - \omega_<) = 0, \tag{30b}$$

where

$$\omega_> = \max[\omega_e(P_0, M_0), \omega_m(P_0, M_0)] \quad \text{and} \quad \omega_< = \min[\omega_e(P_0, M_0), \omega_m(P_0, M_0)], \tag{30c}$$

with

$$\omega_e(P_0, M_0) \equiv -U_e - \mu_e n_e D_e k_e^2 = -\mu_e \left[A^E + \frac{n_e}{\varepsilon} + (3B^E + 2n_e \alpha_p^E) P_0^2 + 6C^E P_0^5 + n_e D_e k_e^2 \right],$$

$$\omega_m(P_0, M_0) \equiv -U_m - \mu_m n_m D_m k_m^2 = -\mu_m [A^M + (3B^M + 2n_m \alpha_m^M) M_0^2 + n_m D_m k_m^2]. \tag{31}$$

Note here that the coupling of P_0 and M_0 comes from A^E and A^M [see Eqs. (19) and (22)]. The constants k_e and k_m are determined from the following pair of transcendental equations derived from the boundary conditions in Eq. (27):

$$\tan\left(\frac{k_e h_e}{2}\right) = \frac{1}{k_e \delta_e} \quad \text{and} \quad \tan\left(\frac{k_m h_m}{2}\right) = \frac{1}{k_m \delta_m}. \tag{32}$$

Clearly, Eq. (30b) shows that the system has two bifurcation points with critical condition $\omega_> = 0$ or $\omega_< = 0$ for phase changes to occur in the respective layers. Depending on the initial stationary state (P_0, M_0), and the direction of heating/cooling, either one can occur first. For example, at a sufficiently high temperature T, both $\omega_>$ and $\omega_<$ are negative [see Eq. (31)] and the paraelectric and paramagnetic states are both stable. As T decreases, $\omega_>(0,0)$ first vanishes and then turns positive at a critical temperature T_{c1}. At this point, any small perturbation grows exponentially beyond all bounds, and the system becomes unstable and bifurcates, undergoing a phase transformation. Thus, when critical conditions are met, the initially stable parastate (with a negative $\omega_>$) transforms into a ferrostate.

To facilitate further discussion, we shall be specific and assume, without loss of generality, that $\omega_>(0,0) = \omega_e(0,0)$; i.e., the ferroelectric transformation occurs at a higher temperature. Then, after the first bifurcation, the system takes on a new configuration, with ferroelectric layers that are electrically polarized. Further cooling turns $\omega_< = \omega_m[P(T_{c2}), 0]$ positive at some temperature $T_{c2} < T_{c1}$, and the corresponding ferromagnetic transformation takes place. The critical condition $\omega_e(0,0) = 0$ of the higher-temperature bifurcation defines a relation among critical parameters for the ferroelectric layers, such as supercooling transition temperature T_{c1}, electric field, applied stress, and system geometry (thicknesses of the films and the substrate). The critical condition $\omega_m[P(T_{c2}), 0] = 0$ then yields the critical properties of the lower-temperature bifurcation, such as phase transition temperature and Curie–Weiss relation of the ferromagnetic layers.

To evaluate the condition $\omega_< = 0$ for the lower-temperature bifurcation from Eq. (31), the stable state of the system after the first bifurcation has to be defined as a function of environmental parameters such as temperature, applied stress, and electric or magnetic fields. It can be determined by solving the steady-state version of Eqs. (18) and (21). The conditions for the higher- and lower-temperature bifurcations $\omega_> = 0$ and $\omega_< = 0$ thus determine the characteristics of the supercooling phase transitions of the system, such as the critical temperatures, critical thicknesses, and Curie–Weiss relations. Similarly, the characteristics of the

superheating phase transitions of the system is determined by the first and second bifurcations $\omega_<=0$ and $\omega_>=0$, respectively.

It is of practical interest to note that a system operating near the second bifurcation exhibits the strongest magnetoelectric effect. For such a system, manipulation of the polarization (magnetization) in the ferroelectric (ferromagnetic) layers can be used to control the stability of the magnetic (electric) state of the other component, thus allowing the magnetization to respond to an electric (magnetic) input via the Curie–Weiss law, and vice versa. The physical principle underlying this statement is illustrated as follows: That the Curie temperature in a ferromagnetic material depends on the applied stress is well established as an inverse magnetostrictive effect. At the same time, the application of an electric field on the ferroelectric layer can induce a sufficiently large electrostrictive stress, which, when transmitted to the ferromagnetic layer, can cause a shift in the ferromagnetic Curie temperature T_{c2}. This can produce a significant change in the magnetization according to the Currie–Weiss law, if allowed to operate at a temperature near T_{c2}. This can be easily seen from the high sensitivity of the magnetization near the Curie temperature. In the specific case when the two Curie temperatures are both close to the operating temperatures, i.e., $T_{c1} \approx T_{c2}$, the effect discussed in the foregoing will be even more magnified due to the Curie–Weiss law in the susceptibilities of both layers. However, it is at the same time much more complicated because of the coupling between the phase transitions in the two layers.

In general, due to the large difference among the quantities $\omega_m(0,0)$, $\omega_m(0,M)$, $\omega_m(P,0)$, and $\omega_m(P,M)$ and $\omega_e(0,0)$, $\omega_e(0,M)$, $\omega_e(P,0)$, and $\omega_e(P,M)$, the system behavior during heat-up and cool-down, or under an applied oscillation field (elastic, electric, and magnetic) would be very complex but, exactly because of that, very interesting.

Before finishing this section, we note that the bifurcation conditions also depend on the thicknesses of the layers, particularly the substrate, via the values of k_e and k_m from Eq. (32). On the other hand, the magnetoelectric effect due to the coupled elastic interaction will change the phase transition temperatures. k_e and k_m, from Eq. (22), can take on infinitely many values. The meaningful solution is the one corresponding to the smallest values of k_e and k_m.

IV. CRITICAL TEMPERATURES FOR BATIO$_3$/EUO

As a simple example to demonstrate the foregoing discussion, we consider a multilayer structure composed of alternating layers (ten each) of ferroelectric $BaTiO_3$ and ferromagnetic EuO on a $SrTiO_3$ (001) substrate (Fig. 1). The material parameters used in the calculation are listed in Table I. For the ferromagnetic layer, the parameters A_m and δ_m are obtained by fitting to the *ab initio* calculation.[23] We note that in the present model, the ferroelectric and ferromagnetic phase transitions are decoupled if the substrate is rigid or thick ($H \to \infty$). Starting from an initial state in which all layers of the system are in the parastate, i.e., $P_0=0=M_0$, Figs. 2 and 3 show the respective ferroelectric and ferromagnetic transition temperatures for different thicknesses of the substrate in the absence of misfit stresses, the ferroelectric and ferromagnetic layers being assumed to have equal thicknesses. We note that in this case, as the substrates get thinner, the ferroelectric or ferromagnetic transformation occurs more easily and at higher temperatures. It can be seen that the former is higher than the latter in all cases under consideration. Furthermore, it also shows that the transition temperatures decrease as expected with decreasing film thicknesses. In Fig. 4, we compare the critical temperatures of ferromagnetic transition (treated as a second bifurcation) with and without the misfit stresses. The 300% increase in the transition temperature clearly shows the strong effect of the coupling of the misfit stresses presently considered. Figure 5 shows the magnetoelectric effect on the para-/ferromagnetic

TABLE I. Material data for model calculation (Refs. 25–27).

$BaTiO_3$ [a] (cgs unit)	$A_e \times 10^{-5}$	7.4
	$D_e \times 10^{-15}$ (cm^2)	3.0
	T^E_{c0} (K)	397
	C^E_{11}	17.55
	$C^E_{12} \times 10^{11}$	8.46
	ε^{0E}_{11}	0.02
	Q (SI)	−0.043
	δ_e (nm)	4
	P_s (esu/cm^3)	78 000
EuO[b] (cgs unit)	A^*_m	0.034
	$D_m \times 10^{-14}$ (cm^2)	5.15
	T^M_{c0} (K)	69.15
	$C^M_{11} \times 10^{12}$	1.79
	$C^M_{12} \times 10^{12}$	0.77
	ε^{0M}_{11}	0.02
	$\lambda \times 10^{-6}$	−20
	M_s (emu/cm^3)	1049
	δ_m (nm)	8
$SrTiO_3$ [c] (cgs unit)	$C^0_{11} \times 10^{12}$	3.16
	$C^0_{12} \times 10^{12}$	1.02

[a]Reference 25.
[b]Reference 26.
[c]Reference 27.

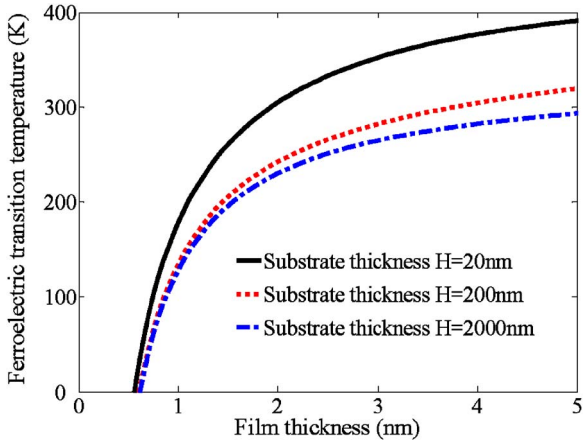

FIG. 2. (Color online) Ferroelectric transition temperature vs the thickness of the ferroelectric layer under different substrate thicknesses in the absence of misfit stresses.

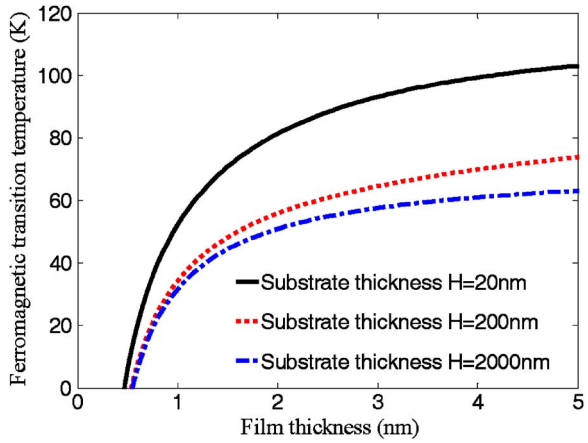

FIG. 3. (Color online) Ferromagnetic transition temperature vs the thickness of the ferroelectric layer under different substrate thicknesses in the absence of misfit stresses.

transition temperature (the second bifurcation) when the polarization (78 000 esu/cm^3) is turned on and off. The large shift in the transition temperature will produce a large change in the magnetic susceptibility via the Curie–Weiss relation. The substrate thickness considered here is 50 nm. We note that some of the material parameters used in this calculation are only provisional, and the results obtained may not represent very well the material system being considered. Nevertheless, our aim to gain an insight into the magnetoelectric effect of the multiferroic-layered system we are considering seems to have been achieved.

V. CONCLUDING REMARKS

In this paper, the critical behavior of a multilayered system of alternating ferroelectric and ferromagnetic thin films on a compliant substrate is analytically modeled. A thermodynamic approach is adopted based on a formulation using the Ginzburg–Landau free energies of the bulk materials. The magnetoelectric coupling due to the interlayer elastic interaction on the critical behavior of the multilayer system is demonstrated and is found to increase with the elastic compliance of the substrate. The system is characterized by two bifurcation points. The system is found to exhibit the strongest magnetoelectric effect at the second bifurcation (i.e., first and second bifurcations in the context of the order of occurrence).

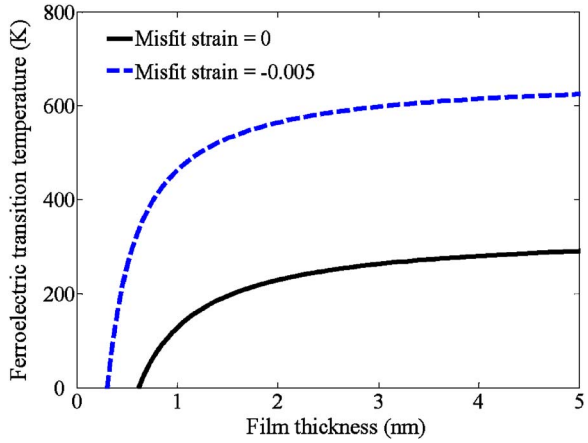

FIG. 4. (Color online) Ferromagnetic transition temperature vs the thickness of the ferroelectric layer with and without the misfit stresses.

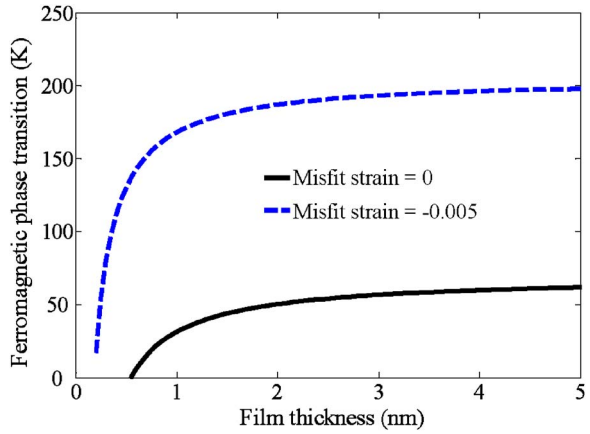

FIG. 5. (Color online) Ferromagnetic transition temperature vs the thickness of the ferroelectric layer with and without the ferroelectric transition.

As an example, a multilayer structure of $BaTiO_3/EuO/SrTiO_3$ is studied under the supercooling conditions. Since its ferroelectric transition temperature is much higher than the ferromagnetic transition temperature in this case, only the effect of the ferroelectric transition on the ferromagnetic transition is investigated. The significant effect of the elastic coupling on the transition temperatures of the ferromagnetic layers due to the ferroelectric transition is shown.

ACKNOWLEDGMENTS

This project was supported by grants from the Research Grants Council of the Hong Kong Special Administrative Region (Grant No. PolyU5322/04E). One of us (B.W.) also wants to thank National Natural Science Foundation of China (Grant Nos. 10572155 and 10732100) for support.

APPENDIX: DERIVATION OF EQUATIONS (18) AND (21)

According to the definition of the variational derivative of a functional,[28] one knows if the variation of a functional

$$I[y(\vec{x})] = \int \int_V \int F[y(\vec{x}), y'(\vec{x})] d\vec{x} \tag{A1}$$

can be written as

$$\delta I = \int \int_V \int g(\vec{x}) \delta y(\vec{x}) d\vec{x}. \tag{A2}$$

Then the functional derivative of I is

$$\frac{\delta I}{\delta y(\vec{x})} = g(\vec{x}). \tag{A3}$$

The total energy of the system is given by Eq. (17) as follows:

$$\Phi = f_P + f_M + f_{\mathrm{el}} + f_\Sigma. \tag{A4}$$

One needs to obtain the function $g(\vec{x})$ to derive the variational derivative. It is easy to get the first variation of f_P, f_M, and f_Σ from Eqs. (1), (2), and (16), respectively. For the elastic energy

$$f_{\mathrm{el}} = \frac{1}{2} n_e \mathbf{C}^E \int_{-h_e/2}^{h_e/2} (\boldsymbol{\varepsilon}^{0E} - \boldsymbol{\varepsilon}^{Et} + \boldsymbol{\varepsilon}^S)^2 dz + \frac{1}{2} n_m \mathbf{C}^M \int_{-h_m/2}^{h_m/2} (\boldsymbol{\varepsilon}^{0M} - \boldsymbol{\varepsilon}^{Mt} + \boldsymbol{\varepsilon}^S)^2 dz + \frac{1}{2} H \mathbf{C}^0 (\boldsymbol{\varepsilon}^S)^2, \tag{A5}$$

one can derive

$$\delta_P f_{\mathrm{el}} = n_e \mathbf{C}^E \int_{-h_e/2}^{h_e/2} (\boldsymbol{\varepsilon}^{0E} - \boldsymbol{\varepsilon}^{Et} + \boldsymbol{\varepsilon}^S) \delta_P (\boldsymbol{\varepsilon}^{0E} - \boldsymbol{\varepsilon}^{Et} + \boldsymbol{\varepsilon}^S) dz + n_m \mathbf{C}^M \int_{-h_m/2}^{h_m/2} (\boldsymbol{\varepsilon}^{0M} - \boldsymbol{\varepsilon}^{Mt} + \boldsymbol{\varepsilon}^S) \delta_P (\boldsymbol{\varepsilon}^{0M} - \boldsymbol{\varepsilon}^{Mt} + \boldsymbol{\varepsilon}^S) dz + H \mathbf{C}^0 \boldsymbol{\varepsilon}^S \delta_P \boldsymbol{\varepsilon}^S. \tag{A6}$$

The substitution of the expressions $\boldsymbol{\varepsilon}^{0E}$, $\boldsymbol{\varepsilon}^{0M}$, $\boldsymbol{\varepsilon}^{Et}$, $\boldsymbol{\varepsilon}^{Mt}$, and $\boldsymbol{\varepsilon}^S$ of Eq. (12) into Eq. (A6) yields Eq. (13) as follows:

$$\delta_P \boldsymbol{\varepsilon}^s = 2 n_e Q \boldsymbol{\Xi} \mathbf{C}^E \int_{-h_e/2}^{h_e/2} P \delta P dz. \tag{A7}$$

One can derive

$$\begin{aligned}
\delta_P f_{el} &= n_e \mathbf{C}^E \int_{-h_e/2}^{h_e/2} (\boldsymbol{\varepsilon}^{0E} - \boldsymbol{\varepsilon}^{Et} + \boldsymbol{\varepsilon}^s) \delta_P (-\boldsymbol{\varepsilon}^{Et} + \boldsymbol{\varepsilon}^s) dz \\
&+ n_m \mathbf{C}^M \int_{-h_m/2}^{h_m/2} (\boldsymbol{\varepsilon}^{0M} - \boldsymbol{\varepsilon}^{Mt} + \boldsymbol{\varepsilon}^s) \delta_P \boldsymbol{\varepsilon}^s dz \\
&+ H \mathbf{C}^0 \boldsymbol{\varepsilon}^s \delta_P \boldsymbol{\varepsilon}^s = -2 n_e Q \mathbf{C}^E \int_{-h_e/2}^{h_e/2} (\boldsymbol{\varepsilon}^{0E} - \boldsymbol{\varepsilon}^{Et} \\
&+ \boldsymbol{\varepsilon}^s) P \delta P dz + 2 n_e Q \boldsymbol{\Xi} \mathbf{C}^E \Bigg[n_e \mathbf{C}^E \int_{-h_e/2}^{h_e/2} (\boldsymbol{\varepsilon}^{0E} - \boldsymbol{\varepsilon}^{Et} \\
&+ \boldsymbol{\varepsilon}^s) dz + n_m \mathbf{C}^M \int_{-h_m/2}^{h_m/2} (\boldsymbol{\varepsilon}^{0M} - \boldsymbol{\varepsilon}^{Mt} + \boldsymbol{\varepsilon}^s) dz \\
&+ H \mathbf{C}^0 \boldsymbol{\varepsilon}^s \Bigg] \int_{-h_e/2}^{h_e/2} P \delta P dz = \Big[-2 n_e Q \mathbf{C}^E \boldsymbol{\varepsilon}^{0E} \\
&+ 2 n_e Q \mathbf{C}^E (h_e \boldsymbol{\Xi} \mathbf{C}^E \boldsymbol{\varepsilon}^{0E} \\
&+ h_m \boldsymbol{\Xi} \mathbf{C}^M \boldsymbol{\varepsilon}^{0M}) \Big] \int_{-h_e/2}^{h_e/2} P \delta P dz \\
&+ 2 n_e Q^2 \mathbf{C}^E \int_{-h_e/2}^{h_e/2} P^3 \delta P dz \\
&+ 2 n_e Q \mathbf{C}^E (n_e \boldsymbol{\Xi} \mathbf{C}^E Q \langle P^2 \rangle \\
&+ n_m \boldsymbol{\Xi} C^M Q_M \langle M^2 \rangle) \int_{-h_e/2}^{h_e/2} P \delta P dz
\end{aligned} \tag{A8}$$

by using the applied force

$$n_e \mathbf{C}^E \int_{-h_e/2}^{h_e/2} (\boldsymbol{\varepsilon}^{0E} - \boldsymbol{\varepsilon}^{Et} + \boldsymbol{\varepsilon}^s) dz + n_m \mathbf{C}^M \int_{-h_m/2}^{h_m/2} (\boldsymbol{\varepsilon}^{0M} - \boldsymbol{\varepsilon}^{Mt} + \boldsymbol{\varepsilon}^s) dz + H \mathbf{C}^0 \boldsymbol{\varepsilon}^s = 0.$$

[1] D. N. Astrov, Sov. Phys. JETP **11**, 708 (1960).
[2] N. A. Hill, J. Phys. Chem. B **104**, 6694 (2000).
[3] A. Filippetti and N. A. Hill, Phys. Rev. B **65**, 195120 (2002).
[4] J. van Suchtelen, Philips Res. Rep. **27**, 28 (1972).
[5] G. Srinivasan, E. T. Rasmussen, B. Levin, and R. Hayes, Phys. Rev. B **65**, 134402 (2002).
[6] S. X. Dong, J. R. Cheng, J. F. Li, and D. Viehland, Appl. Phys. Lett. **83**, 4812 (2003).
[7] J. Wang, J. B. Neaton, H. Zheng, V. Nagarajan, S. B. Ogale, B. Liu, D. Viehland, V. Vaithyanathan, D. G. Schlom, U. V. Waghmare, N. A. Spaldin, K. M. Rabe, M. Wutlig, and R. Ramesh, Science **299**, 1719 (2003).
[8] H. Zheng, J. Wang, S. E. Lofland, Z. Ma, L. Mohaddes-Ardabili, T. Zhao, L. Salamanca-Riba, S. R. Shinde, S. B. Ogale, F. Bai, D. Viehland, Y. Jia, D. G. Schlom, M. Wuttig, A. Roytburd, and R. Ramesh, Science **303**, 661 (2004).
[9] D. V. Efremov, J. Van Den Brink, and D. I. Khomskii, Nat. Mater. **3**, 853 (2004).
[10] M. Fiebig, Th. Lottermoser, D. Frohlich, A. V. Goltsev, and R. V. Pisarev, Nature (London) **419**, 818 (2002).
[11] J. B. Neaton, C. Ederer, U. V. Waghmane, N. A. Spaldin, and K. M. Rabe, Phys. Rev. B **71**, 014113 (2005).
[12] C. Ederer and N. Spaldin, Phys. Rev. B **71**, 060401 (2005).
[13] B. B. Van Aken, T. T. M. Palstra, A. Filippetti, and N. A. Spaldin, Nat. Mater. **3**, 164 (2004).
[14] P. Murugavel, D. Saurel, W. Prellier, Ch. Simon, and B. Raveau, Appl. Phys. Lett. **85**, 4424 (2004).
[15] P. Murugavel, M. P. Singh, W. Prellier, B. Mercey, Ch. Simon, and B. Raveau, Appl. Phys. Lett. **97**, 103914 (2005).
[16] C.-W. Nan, G. Liu, Y. Lin, and H. Chen, Phys. Rev. Lett. **94**, 197203 (2005).
[17] Y. Lin, N. Cai, J. Zhai, G. Liu, and C.-W. Nan, Phys. Rev. B **72**, 012405 (2005).
[18] B. Wang and C. H. Woo, J. Appl. Phys. **100**, 044114 (2006).
[19] C. H. Woo and Y. Zheng, Appl. Phys. A: Mater. Sci. Process. **91**, 59 (2008).
[20] S. P. Timoshenko and J. N. Gooier, *Theory of Elasticity* (McGraw-Hill, New York, 1970).
[21] P. G. de Gennes, *Superconductivity of Metals and Alloys* (Addison-Wesley, Reading, MA, 1989).
[22] D. Schwenk, F. Fishman, and F. Schwabl, J. Magn. Magn. Mater. **93**, 80 (1991).
[23] R. Schiller and W. Nolting, Phys. Rev. Lett. **86**, 3847 (2001).
[24] E. Weschke, H. Ctt, E. Schierle, C. Schüßler-Langeheine, D. V. Vyalikh, G. Kaindl, V. Leiner, M. Ay, T. Schmitte, and H. Zabel, Phys. Rev. Lett. **93**, 157204 (2004).
[25] S. Li, J. A. Eastman, J. M. Vetrone, C. H. Foster, R. E. Newnham, and L. E. Cross, Jpn. J. Appl. Phys., Part 1 **36**, 5169 (1997).
[26] F. Holtzberg, T. R. McGuire, and S. Methfessel, *Compounds with Lanthanide and Actinide Elements of Some Special Structure Types*, Landolt-Bornstein, New Series, Group III, Vol. 4, Pt. A (Springer-Verlag, Berlin, 1970), pp. 64–109.
[27] J. D. Huang, M. H. Kook, H. S. Lim, and S. C. Ng, J. Appl. Phys. **94**, 7341 (2003).
[28] I. M. Gelfand and S. V. Fomin, *Calculus of Variations* (Prentice-Hall, Englewood Cliffs, NJ, 1963), pp. 27–31.